Nonlinear Behaviour of Cappadocia Tuff Stone Masonry Shear Walls

Burcu Dinç-Şengönül[1] (✉), Rita Esposito[2], and Nabi Yüzer[1]

[1] Department of Environmental Engineering, Faculty of Civil Engineering, Yildiz Technical University, Davutpasa Campus, 34220 Esenler, Istanbul, Turkey
bdinc@yildiz.edu.tr

[2] Faculty of Civil Engineering and Geosciences, Delft University of Technology, Stevinweg 1, 2628 CN Delft, the Netherlands

Abstract. Anatolia has been home to various long-standing civilizations, many of which have left historical monuments for future generations. The Cappadocia area, which covers over 5000 km^2 in Central Anatolia, Turkey, is home to several rock-cut constructions and masonry buildings built of tuff stone. Preserving these monuments, listed as UNESCO World Heritage sites, is critical for the region. This study focuses on the in-plane behavior of walls constructed of tuff stone and alkali-activated waste earth mortar, which is typical in the Cappadocia region. First, an experimental investigation is described. Second, a simplified block-based modeling technique is used to perform 3D nonlinear finite element analysis, which replicates the experimental results. The findings of the numerical modeling approach were then compared to experimental data, emphasizing the lateral load-displacement response of masonry tuff stone walls. There was good agreement between the experimental and numerical results.

Keywords: Cappadocia region · Tuff stone masonry · Alkali-activated mortar · Nonlinear finite element analysis · Block-based modelling

1 Introduction

The Cappadocia Region's historical structures and natural landscapes have been designated mixed heritage sites on the World Heritage List since 1985 [1–4]. Because of its numerous benefits, rock-hewn facilities, particularly rock-cut warehouses, have grown in popularity over the last 30 years. Rock-cut buildings serve a variety of uses, but their primary role is to store fruits and vegetables. These structures continue to be constructed for this function. The rock-cut and masonry constructions in the region show various signs of deterioration induced by both natural and human forces. According to the investigations, the most common types of damage found in the region's rock-cut buildings are capillary cracks and deep structural cracks created on the surface due to rock formation characteristics, disasters, and ground settlement [4–8]. Because these damages are directly connected to the emphasis on the structure, numerical analysis is required to examine their complex and nonlinear behavior.

G. Milani and B. Ghiassi (Eds.): IB2MaC 2024, LNCE 613, pp. 163–174, 2024.
https://doi.org/10.1007/978-3-031-73314-7_12

Using tuff stone masonry as a building material has a prolonged and widespread history. It was employed by the Romans to construct monuments, bridges, aqueducts, palaces, and other buildings. It entails using mortar joints to arrange tuff stones in a consistent pattern. Prevalent were tuff stones in seismically active regions like Turkey, Italy, and Japan. Extensive experimental and theoretical research is available for different types of masonry [9–17]. Nevertheless, further research is still needed to fully understand the mechanical behavior of tuff stone masonry from an experimental, numerical, and analytical perspective. Furthermore, no research has been done in the literature on the behavior of walls constructed with the traditional tuff stone of the Cappadocia region and alkali-activated Cappadocia waste earth mortar.

Presenting an efficient modeling process for the tuff stone masonry walls under in-plane shear compression is the primary goal of this work. For this reason, in the Yildiz Technical University laboratory, tuff stone masonry walls were created using traditional Cappadocian tuff stones and alkali-activated Cappadocia waste earth mortar. These walls have been subjected to tests with shear compression to assess the nonlinear behavior of walls made of tuff stone. Then, in order to simulate this experimental investigation, nonlinear analyses were carried out. A 3D simplified block-based modeling method was adopted. The numerical results showed good agreement with the experimental one both in term of maximum base shear force and initial stiffness. These findings are crucial for future research on assessing grout injection's efficacy as a repair technique.

2 Experimental Procedure

Cappadocia waste earth (CWE) was obtained from the excavation earth of rock-cut structures in Cappadocia (Nevşehir) to produce alkali-active mortar. Additionally, air-slaked lime (CL 80-S), known as calcium hydroxide (CH), was a secondary precursor in mortar mixes that met the EN 459–1 standard. CWE was dry milled and sieved to obtain a grain size of <63 μm, which improved its reactivity for alkali activation. The primary alkaline activators in this context were sodium hydroxide, indicated as NaOH (NH), and sodium silicate, usually referred to as waterglass (WG) (with a $M_s = SiO_2/Na_2O$ molar ratio of 3.37). The water-to-binder ratio was set at 0.55. This study used traditional Cappadocian tuff stones to construct tuff stone masonry walls. Tables 1 and 2 show the mechanical characteristics of mortar and stone units, respectively [8].

Table 1. Mechanical properties of mortar.

Material	28th day		90th day			
	Flexural strength, MPa	Compressive strength, MPa	Tensile strength, MPa	Compressive strength, MPa	Modulus of elasticity, MPa	Poisson's ratio
Mortar	0.6	1.9	0.4	2.1	820	0.10

The stone masonry test walls (1010x1005x280 mm) were built to investigate the in-plane behavior of tuff stone masonry walls. The test walls were tested 150 days after

Table 2. Mechanical properties of stone.

Material	Modulus of Elasticity, MPa	Poisson's ratio	Compressive strength, MPa	Flexural strength, MPa	Tensile strength,MPa
Stone	1100	0.22	6.5	0.7	0.6

construction with an incremental lateral load and a constant, uniformly distributed vertical load. The loading instrumentations comprised hydraulic rams with capacities of 2000 kN for vertical loading and 500 kN for horizontal loading. The selection of the pre-compression level at 0.7 MPa (200 kN vertical load) for the test remained consistent. It was determined by referencing prior experimental studies in the literature and the characteristics of walls in existing structures in the Cappadocia region. A vertical hydraulic jack coupled to a steel frame was used to compress the test walls. A robust steel beam linked to the jack distributed the pre-compression force equally. Furthermore, a steel plate hung from the steel beam by steel cables transmitted the vertical weight to the top of the wall. The vertical movement was unfettered because there was no connection between the steel plate and the higher course of blocks, assuring complete contact with the wall's top. The top steel plate was restrained from rotating about its axes and translating out of the plane. At the commencement of the test, the vertical apparatus dropped to apply the appropriate pre-compression load. The vertical movement of the beam and plate was then limited, and the lateral force was applied using the horizontal loading jack. The horizontal and vertical actuators were both load controlled. The lateral loading rate was 0.60.1 kN/s. Each wall was constructed on a solid steel plate firmly fastened to a steel foundation within the loading frame. Linear variable displacement transducers (LVDT) were used as measuring tools. Additionally, potentiometric position transducers were used to measure the lateral displacements of the upper and lower parts of the walls. Figure 1 depicts the experimental test setup, which includes a data-gathering device that captures all test data at the same time. The masonry stone walls remained repetitious and similar in each test iteration, and the test concluded when a stair-step crack developed diagonally across the wall. The specimens were not allowed to reach the near-collapse state (e.g., a 20% reduction in base shear force after the peak) to maintain their integrity for the investigation of repair methods [18].

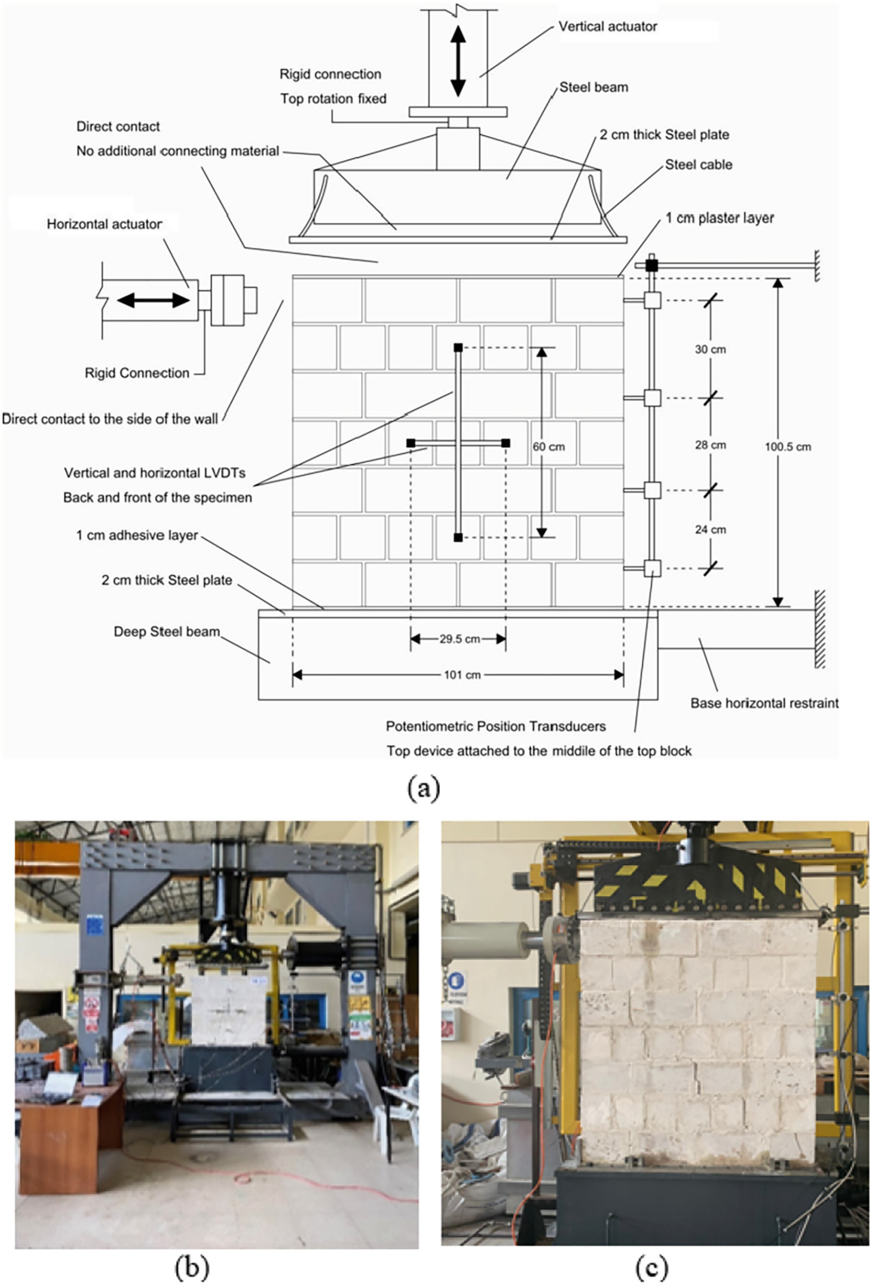

Fig. 1. (a) Test set-up (b) Before the wall test (c) After the wall test.

3 Numerical Modeling

A 3D model was created using linear solid components and linear surface interface elements (Fig. 2). In the simplified block-based technique, the stone was represented as a solid block (expanded in geometry) [19]. At the same time, interface components were used to represent mortar joints, stone-joint connections, and probable fissures in the stone just above the site of head joints. Solid components were also employed to represent the upper steel beam. An average mesh size of 72 mm was used.

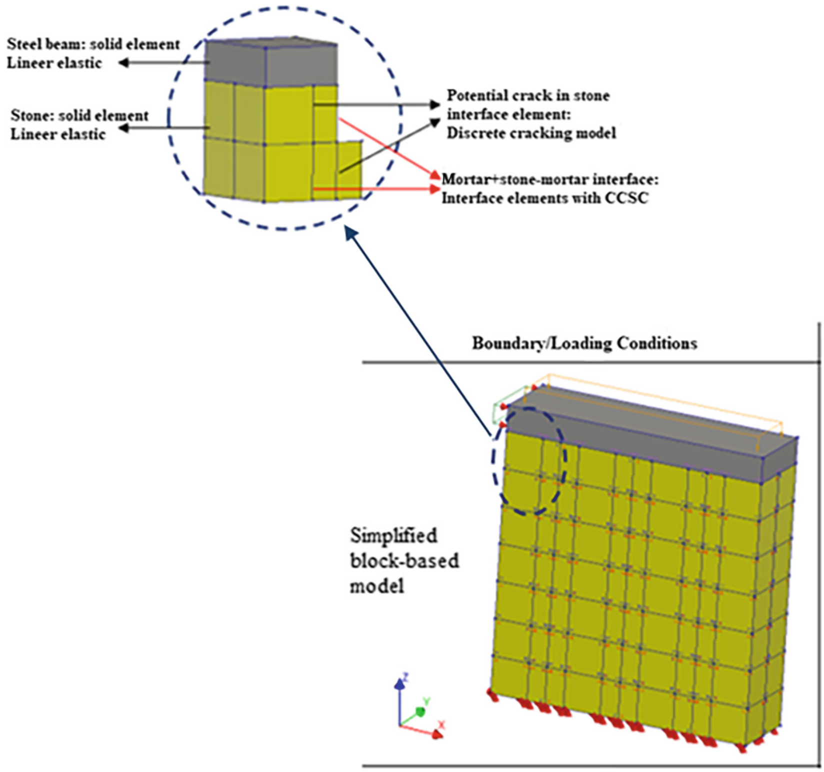

Fig. 2. Details of finite element model.

A phased analysis was used to simulate the experiment. The self-weight and vertical load were applied in the first phase, followed by the in-plane lateral load in the second. Both loads were applied in displacement control, considering that the vertical displacement (along the Z-axis) remained constant after the first phase during the experiment. The z-direction translation (u_z) on the top surface was limited during the second phase. The second phase's pushover load was applied to nodes on the top beam's left edge using a monotonically rising prescribed deformation in the x-direction (u_x). The wall's foundation was limited in all translational degrees of freedom. The vertical load was applied in the first phase, and displacement remained constant throughout the analysis.

All numerical studies used a Secant (Quasi-Newton) iteration approach with 10^{-2} tolerance for displacement and force norm convergence controls. Also, the experiments (up to 15 mm displacement) and then the near collapse state (up to 50 mm displacement) were simulated.

Mortar joints and stone-mortar connections were classified as zero-thickness interface components in the 3D simplified block-based model technique. Simultaneously, stones were increased in geometry and represented with solid components. Material nonlinearity was only examined in contact parts that used the Combined Cracking-Shearing-Crushing (CCSC) material model [20]. This material model can represent both tensile and shear sliding failures in mortar or stone-mortar bonding and mortar compressive failure [21]. An exponential softening was examined in tension and shear, whereas compression was chosen using a parabolic curve [22, 23].

The 3D block-based model explicitly represents stone and mortar joints with solid components and interface elements. The material nonlinearity of the interface elements was investigated using the CCSC model. A discrete cracking model with linear tension softening was used to simulate the stone tensile failure, with vertical interface components introduced in regions below and above the head joint. The solid stone components were maintained linearly stretchy. The solid parts representing the steel beam also maintained linear elasticity since the beam was significantly stiffer and more robust than the brick wall. Table 3 summarizes material attributes for the 3D simplified block-based models.

Figure 3 compares the experimental and numerical results in terms of load-displacement responses. The numerical model gives good agreement regarding the lateral force vs displacement curve. However, the numerical findings are closer to the upper bound provided by experiments. This situation is due to the absence of spatial diversity in mechanical characteristics in the model. Both models agree well on initial stiffness and maximum load within the experiment's displacement range. The simplified model closely matches the experimental curve when comparing the data in the 10–15 mm range (the end of the experiment). To assess the numerical in-plane drift capacity and entire post-peak behavior of tuff stone masonry walls, the lateral displacement was extended in the numerical simulations beyond 15 mm (end of tests), as shown in Fig. 3b. The numerical model predicts a comparable maximum base shear force (170 kN for the simplified model).

Table 3. Summary of material parameters for 3D simplified block-based model.

	Parameter	Value	Reference	
Solid elements representing stones (Linear elastic)	Young's modulus, E	1100 N/mm^2	Determined	Uniaxial compression test
	Poisson's ratio, υ	0.22	Determined	Uniaxial compression test
Interface element representing mortar joints and stone-mortar bonds (CCSC)	Normal stiffness modulus, k_{nn}	50 N/mm^3	Calibrated	Flat-jack test
	Shear stiffnesses modulus,k_{tt} and k_{ss}	20 N/mm^3	Calibrated	Flat-jack test
	Tensile strength, f_t	0.2 N/mm^2	Assumed	$f_t = 2/3{*}f_{flexural}$
	Tensile fracture energy, G_{ft}	0.1 N/mm	Assumed	$G_{ft} = 0.025(2f_t)^{0.7}$
	Cohesion, c	0.2 N/mm^2	Assumed	Triaxial compression test
	Friction angle, ϕ	20	Assumed	Triaxial compression test
	Dilatancy angle, ψ	0	Assumed	[24]
	Compressive strength, f_c	8 N/mm^2	Assumed	[25]
	Compressive fracture energy, G_{fc}	25.89 N/mm	Assumed	$G_{fc} = 15 + 0.43f_c$ - $0.0036f_c2$
Interface element representing potential cracks in stones (Discrete cracking)	Normal stiffness modulus, k_n	100 N/mm^3	Assumed	[25]
	Shear stiffness modulus, k_t and k_s	100 N/mm^3	Assumed	[25]
	Tensile strength, f_t	0.6 N/mm^2	Determined	Tensile test
	Fracture energy, G_{ft}	0.3 N/mm	Assumed	[25]

Figure 4 depicts the numerical outputs for the masonry tuff stone walls. Points 1, 2, and 3 were identified as displacement values at 15, 30, and 50 mm, respectively. As predicted, the fractures in the wall samples begin in the top and bottom corners of the wall. The top right and bottom left blocks rotate, causing tensile deformation in the bed joints. The primary mode of wall deformation, shear, begins at the bed joints of all mortar layers and is followed by tensile deformation of the surrounding head joints. The numerical study revealed that the failure mechanism occurred solely in the joints, not on the stones. Furthermore, the rotation of the blocks at the corner has resulted in severe compressive loads and crushing failure in the bed joint areas (Fig. 4b). The simplified block-based model's crack patterns are consistent with those in the experimental tests.

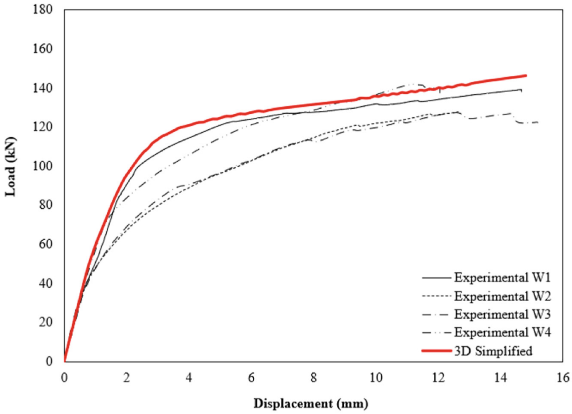

(a)

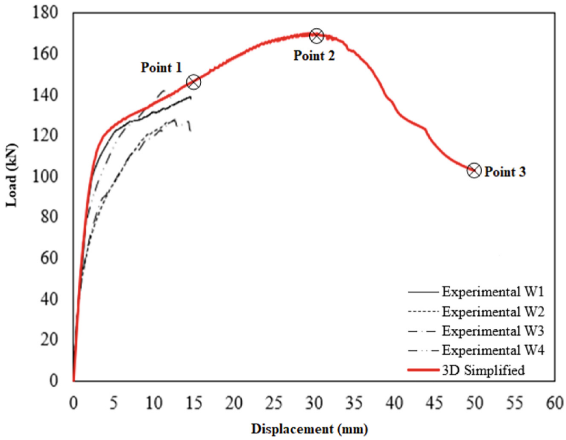

(b)

Fig. 3. (a) Comparison between experimental and numerical load-displacement responses, (b) The numerical in-plane drift capacity of the masonry tuff stone walls.

4 Conclusions

The experimental study focused on evaluating the in-plane behavior of masonry walls built with tuff stone and alkali-activated mortar typical from Cappadocia region. These tests were used as a reference for calibrating the numerical study. By comparing the numerical and experimental capacity, it was determined that the numerical model effectively replicated the in-plane behavior of these walls. The maximum horizontal loads were accurately estimated, and the initial stiffness closely matched the experimental results. In-plane nonlinear behavior of stone walls after grouting will be investigated in future works.

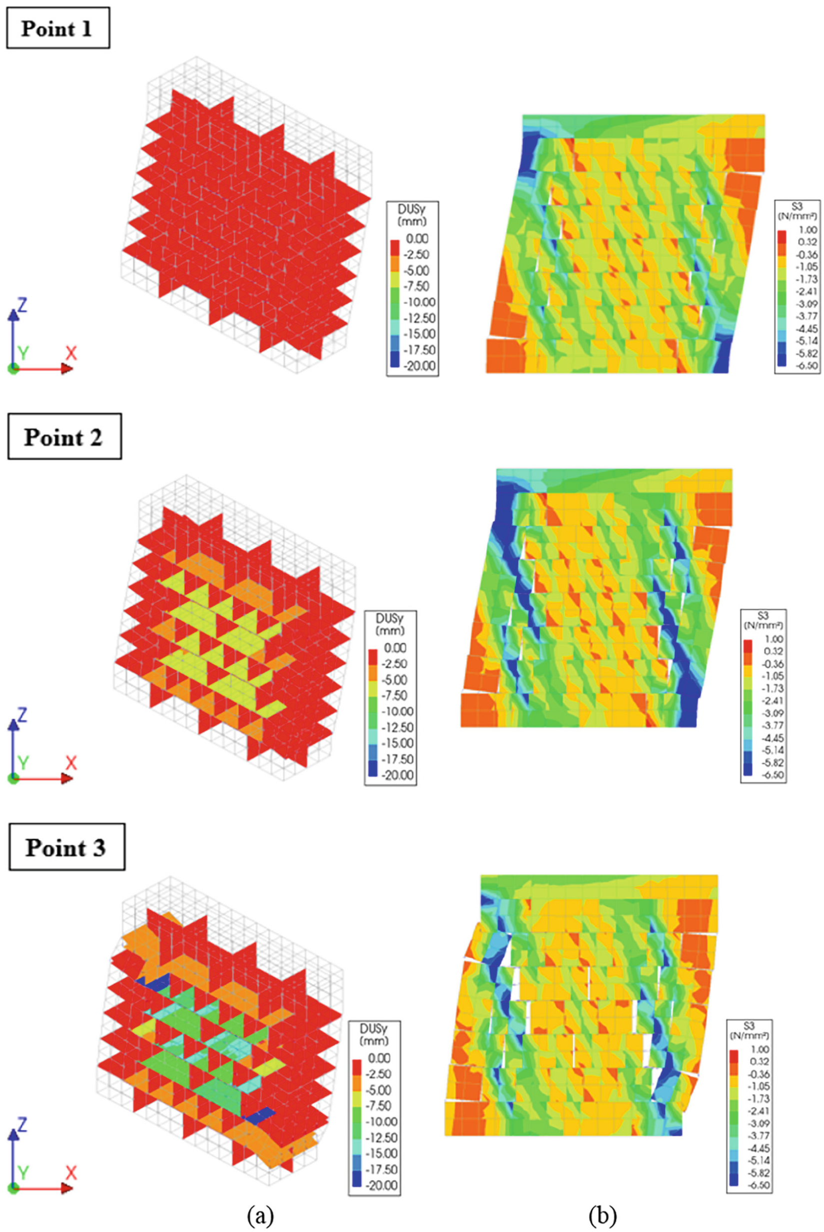

Fig. 4. (a) Sliding in interface elements in the global X-direction (b) Minimum principal stresses in extended stones (c) The normal relative displacement in the interfaces (d) Deformation in X direction.

Acknowledgements. Acknowledgements & Funding. This work was supported by the research grants of The Scientific and Technological Research Council of Turkey [Project No. 118M321] and Yildiz Technical University Research Foundation [Project No. FDK-2021–4781]. The first

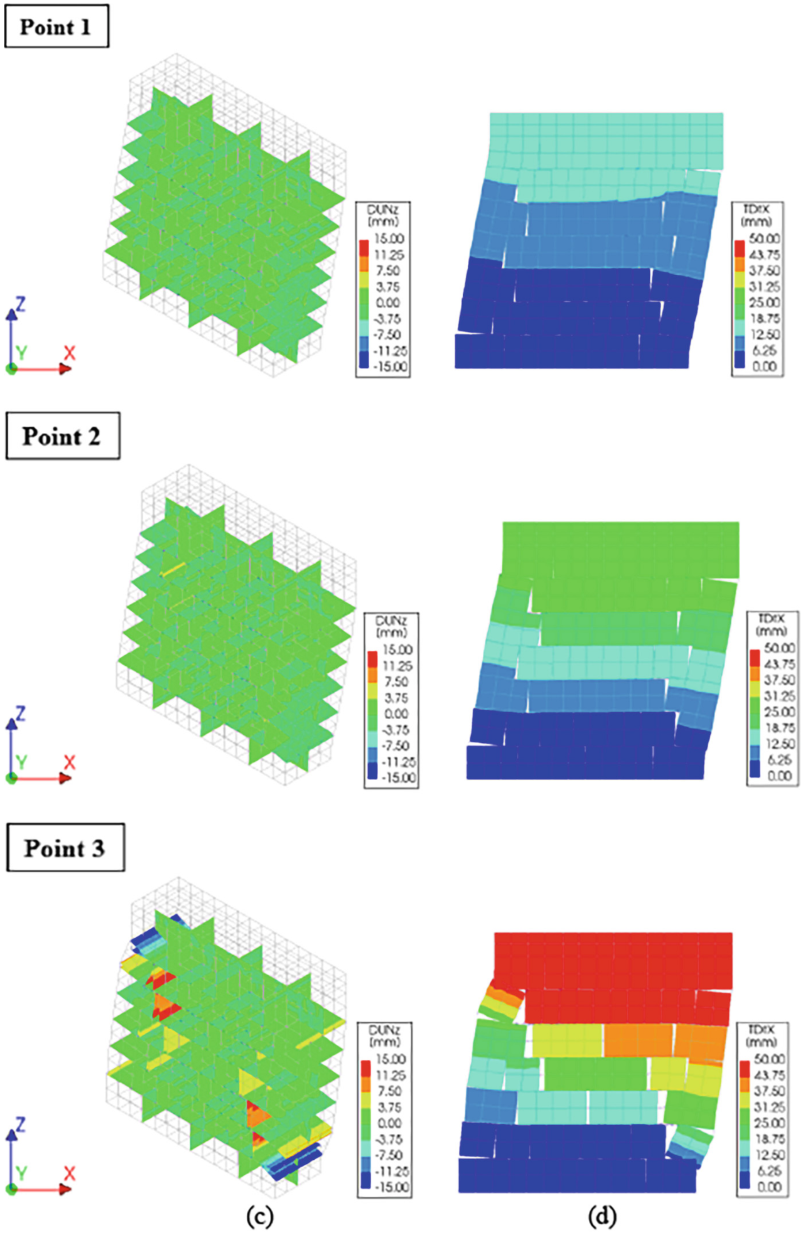

Fig. 4. (*continued*)

author wishes to thank the Scientific and Technological Research Council of Turkey for granting a research fellowship [2214-A-International Research Fellowship Programme for PhD Students], who supported her visiting period at Delft University of Technology.

References

1. Aydan Ö, Ulusay R (2003) Geotechnical and geoenvironmental characteristics of man-made underground structures in Cappadocia. Turkey Eng Geol 69:245–272. https://doi.org/10.1016/S0013-7952(02)00285-5
2. Erguler ZA (2009) Field-based experimental determination of the weathering rates of the Cappadocian tuffs. Eng Geol 105:186–199. https://doi.org/10.1016/j.enggeo.2009.02.003
3. Ulusay R et al (2006) Assessment of environmental and engineering geological problems for the possible re-use of an abandoned rock-hewn settlement in Urgüp (Cappadocia). Turkey, Environ Geol 50:473–494. https://doi.org/10.1007/s00254-006-0222-4
4. Bayram M, Oktay D, Yuzer N (2022) Evaluation of fresh properties and rheological behavior of lime-based grouts with Cappadocia waste earth. Int J Architectural Heritage.https://doi.org/10.1080/15583058.2022.2089071
5. Ozata Ş (2022) Investigating the use of alkali-activated volcanic tuff of Cappadocia region in historic masonry buildings. PhD Thesis. Dept. of Architecture, Yildiz Technical Univ. Turkish
6. Ozata Ş (2015) The problems and possible solutions of rock-cut structures in cappadocia region. Master's Thesis. Dept. of Architecture, Yildiz Technical Univ. Turkish
7. Ozata Ş, Arun G (2018) Damage assessment of rock-cut ortahisar castle in Cappadocia region. Gazi Univ J Sci 31:1–11
8. Ozata S, Akturk B, Yuzer N (2022) Utilization of waste Cappadocia earth as a natural pozzolan in alkali activation: a parametric study. Constr Build Mater, 329.https://doi.org/10.1016/j.conbuildmat.2022.127192
9. Vasconcelos G, Lourenço PB (2009) Experimental characterization of stone masonry in shear and compression. Constr Build Mater 23:3337–3345. https://doi.org/10.1016/j.conbuildmat.2009.06.045
10. Abdel-Mooty M, Al Attar A, El Tahawy M (2011) Experimental evaluation of stone masonry walls with lime-based mortar under vertical loads. WIT Trans Built Environ 118:401–412. https://doi.org/10.2495/STR110331
11. Rezaie A, Godio M, Beyer K (2020) Experimental investigation of strength, stiffness and drift capacity of rubble stone masonry walls. Constr Build Mater 251:118972. https://doi.org/10.1016/j.conbuildmat.2020.118972
12. Giaretton M, Valluzzi MR, Mazzon N, Modena C (2017) Out-of-plane shake-table tests of strengthened multi-leaf stone masonry walls. Bull Earthq Eng 15:4299–4317. https://doi.org/10.1007/s10518-017-0125-7
13. Sandoli A, Ferracuti B, Calderoni B (2019) FRP-confined tuff masonry columns: regular and irregular stone arrangement. Compos B Eng 162:621–630. https://doi.org/10.1016/j.compositesb.2019.01.015
14. Roca P, Viviescas Á, Lobato M, Díaz C, Serra I (2011) Capacity of shear walls by simple equilibrium models. Int J Architectural Heritage 5:412–435. https://doi.org/10.1080/15583058.2010.501481
15. Lignola GP, Prota A, Manfredi G (2009) Nonlinear analyses of tuff masonry walls strengthened with cementitious matrix-grid composites,https://doi.org/10.1061/ASCECC.1943-5614.0000007
16. Prota A, Marcari G, Fabbrocino G, Manfredi G, Aldea C (2006) Experimental in-plane behavior of tuff masonry strengthened with cementitious matrix-grid composites. J Compos Constr 10:223–233. https://doi.org/10.1061/(ASCE)1090-0268(2006)10:3(223)
17. Saviano F, Parisi F, Lignola GP (2022) Material aging effects on the in-plane lateral capacity of tuff stone masonry walls: a numerical investigation. Mater Struct/Materiaux et Constr, 55.https://doi.org/10.1617/s11527-022-02032-5

18. Dinç-Şengönül B, Yüzer N, Şengönül C, Ulukaya S, Oktay D, Ündül Ö (2023) Behavior of grout injected solid stone masonry walls under in-plane loading. Structures 58:105411. https://doi.org/10.1016/j.istruc.2023.105411
19. Drougkas A, Licciardello L, Rots JG, Esposito R (2020) In-plane seismic behaviour of retrofitted masonry walls subjected to subsidence-induced damage. Eng Struct 223:111192. https://doi.org/10.1016/j.engstruct.2020.111192
20. Chang L (2022) Parametric numerical study on two-way bending capacity of unreinforced masonry walls: evaluation of the influence of geometric parameters to improve analytical formulations
21. Schreppers GMA, Garofano A, Messali F, Rots JG (2016) DIANA validation report for masonry modelling. DIANA FEA report
22. Pereira JM, Correia AA, Lourenço PB (2021) In-plane behaviour of rubble stone masonry walls: experimental, numerical and analytical approach. Constr Build Mater 271:121548. https://doi.org/10.1016/j.conbuildmat.2020.121548
23. Haach VG, Vasconcelos G, Lourenço PB (2011) Parametrical study of masonry walls subjected to in-plane loading through numerical modeling. Eng Struct 33:1377–1389. https://doi.org/10.1016/j.engstruct.2011.01.015
24. Augenti N, Parisi F (2011) Constitutive modelling of tuff masonry in direct shear. Constr Build Mater 25:1612–1620. https://doi.org/10.1016/j.conbuildmat.2010.10.002
25. Lee KH (2022) A comparison study of numerical modeling approaches for simulating the in-plane seismic response of masonry walls, Delft University of Technolog